

A Comparative Study of the Parker Instability under Three Models of the Galactic Gravity⁵

Jongsoo Kim^{1,2,3}, and S. S. Hong^{2,4}

ABSTRACT

To examine how non-uniform nature of the Galactic gravity might affect length and time scales of the Parker instability, we took three models of gravity, including the usual uniform one. In a linear model we let the acceleration perpendicular to the Galactic plane increase linearly with vertical distance z from the mid-plane. As a more realistic choice, we let a hyperbolic tangent function of z describe the observationally known variation of the vertical acceleration. To make comparisons of the three gravity models on a common basis, we first fixed the ratio of magnetic pressure to gas pressure at $\alpha = 0.25$, that of cosmic-ray pressure at $\beta = 0.4$, and the *rms* velocity of interstellar clouds at $a_s = 6.4 \text{ km s}^{-1}$, and then adjusted parameters of the gravity models in such a way that the resulting density scale heights for the three models may all have the same value of 160 pc.

In the initial equilibrium state, the vertical density structure is given by an exponential, Gaussian, and power of hyperbolic cosine functions of z for the uniform, linear, and realistic gravity models, respectively. Performing linear stability analyses onto these equilibria with the same ISM conditions specified by the above α , β , and a_s values, we calculate the maximum growth rate and corresponding length scale for each of the gravity models. Under the uniform gravity the Parker instability has the growth time of 1.2×10^8 years and the length scale of 1.6 kpc for symmetric mode. Under the realistic gravity it grows in 1.8×10^7 years for both symmetric and antisymmetric modes, and develops density condensations at intervals of 400 pc for the symmetric mode and 200 pc for the antisymmetric one. A simple change of the gravity model has thus reduced the growth time by almost an order of magnitude and its length scale by factors of four to eight. These results suggest that an onset of the Parker instability in the ISM may not necessarily be confined to the regions of high α and β .

Subject headings: instabilities — ISM: clouds — ISM: magnetic fields — magnetohydrodynamics: MHD

¹Korea Astronomy Observatory, San 36-1, Hwaam-Dong, Yusong-Ku, Taejon 305-348, Korea

²Department of Astronomy, Seoul National University, Seoul 151-742, Korea

³e-mail: jskim@hanul.issa.re.kr

⁴e-mail: sshong@astroism.snu.ac.kr

⁵To appear in the *Astrophysical Journal*, November 1, 1998 issue, Vol. 507

1. INTRODUCTION

By performing linear stability analysis upon an initial equilibrium state of interstellar matter (ISM) that is supported against an externally given uniform gravity by the pressures of interstellar gas, magnetic fields, and cosmic ray particles, Parker(1966) proved that such a system is unstable to long wavelength perturbations along the direction of initial unperturbed magnetic fields. Since then many studies investigated effects on the Parker instability of rotation (Shu 1974; Zweibel & Kulsrud 1975; Foglizzo & Tagger 1994), magnetic microturbulence (Zweibel & Kulsrud 1975), skewed configuration of magnetic fields (Hanawa *et al.* 1992a), non-uniform nature of the externally given gravity (Horiuchi *et al.* 1988; Giz & Shu 1993; Kim *et al.* 1997), self-gravity of the ISM (Elmegreen 1982; Nakamura *et al.* 1991; Hanawa *et al.* 1992b), and the Galactic corona (Kamaya *et al.* 1997). The Parker instability is expected to play significant roles in the dynamo action of accretion disks (Tout & Pringle 1992) and the ejection of mass to galactic halos (Kamaya *et al.* 1996). The instability has been thought an important formation mechanism of the giant molecular cloud complexes (GMCs) in the Galaxy (Appenzeller 1974; Mouschovias *et al.* 1974; Blitz & Shu 1980; Shibata & Matsumoto 1991; Handa *et al.* 1992; Gomez de Castro & Pudritz 1992).

As a formation mechanism of the GMCs, the Parker instability under the uniform gravity is facing two severe problems. The fastest growing mode has an infinite wavenumber along the radial direction, which is the direction perpendicular to both the unperturbed magnetic field and the externally given gravity (Parker 1967). Therefore, small-scale chaotic structures rather than large-scale condensations are likely to form through the instability (Asséo *et al.* 1980; Kim *et al.* 1998). Another problem lies in the time and length scales. If perturbations of finite vertical wavelength are given, at canonical ISM conditions (*cf.* Spitzer 1978), the Parker instability under the uniform gravity grows in a time scale of 1.2×10^8 years with the corresponding length scale being 1.6 kpc. These scales are too long and too large for the Parker instability to be the formation mechanism of the GMCs, since lifetime of interstellar clouds is only about 3×10^7 years (Blitz & Shu 1980) and mean separation of the GMCs is observed to be about 0.5 kpc (Blitz 1991).

In relation to the second problem of scales, Mouschovias *et al.* (1974) pointed out that physical conditions behind the Galactic shocks are more favorable to trigger the Parker instability than in general interstellar space. It is true that in the shocked region one may reduce both scales by significant factors. But at the same time an increase in density there makes heretofore ignored self-gravity important. The Jeans instability would then override the Parker instability (Elmegreen 1982).

The first problem of an infinite wavenumber has its root at the Rayleigh-Taylor instability, whose growth rate increases with increasing wavenumber. Hanawa *et al.* (1992a) sought a solution to this problem of infinite wavenumber from a skewed magnetic field. If the field lines change their directions systematically with height from the Galactic mid-plane, the buoyancy is likely to be suppressed. According to their analysis, the fastest growing mode of the Parker instability

takes a wavelength of $\lambda \simeq 10H$, with H being the density scale height. As long as the skewness is appreciable, for example, more than $30^\circ/H$, the wavelength of maximum growth rate doesn't seem to depend sensitively on the degree of skewness. Observational confirmations are still needed on the skewness of the Galactic magnetic fields. Even if a significant skewness is confirmed, the resulting scale length of $10H$ is again too large for the GMCs. This brings us back to the second problem of scales involved in the perturbations along the field line.

Parker (1966) assumed, in his pioneering study, the vertical gravitational acceleration to be a constant of z . In many ensuing studies the assumption of uniform gravity was almost exclusively employed in estimating the time and length scales of the instability. The values of 1.2×10^8 years and 1.6 kpc we quoted above and $\lambda \simeq 10H$ of Hanawa *et al.* (1992a) are all based on the same assumption of uniform gravity. However, we do know that the Galactic gravity is of non-uniform nature (Oort 1965; Bienaymé, Robin & Crézé 1987, hereafter BRC). It is then interesting to see how much reductions one may achieve in the length and time scales by introducing a realistic model for the Galactic gravity.

The uniform gravity assumption has brought a few unphysical features to the classical picture of the Parker instability. Under a constant acceleration, the equilibrium distribution of density follows an exponential function of height z and has a cusp at the mid-plane, which accompanies a discontinuity in the pressure gradient at $z = 0$. Because of the discontinuity the linear stability analyses based on the uniform gravity ought to be limited to the perturbations of mirror symmetric mode only; while the perturbations of antisymmetric mode are expected to dominate the symmetric ones (Horiuchi *et al.* 1988; Basu *et al.* 1997). The antisymmetric mode would not only slightly increase the growth rate over the value of mirror symmetry, but also obviously reduce the distance between condensations by a factor of two. Therefore, models other than the uniform gravity are required to make better estimations of the time and length scales for the Parker instability in the Galaxy.

In their linear stability analysis, Giz & Shu(1993) introduced a hyperbolic tangent function of z to model the vertical variation of the Galactic gravity. And recently Kim *et al.* (1997) used a linear function of z as a non-uniform model of the Galactic gravity. Both studies demonstrated that dynamical evolution of the perturbations given to the Galactic disk would follow, under such non-uniform gravities, two different families of solutions. They are called *continuum* and *discrete* families. The familiar continuum family has two modes of solutions: One is the original Parker mode, which is a slow magnetohydrodynamic (MHD) mode modulated by the gravity, and the other is a stable Alfvén mode. The newly discovered discrete family has three modes: stable fast MHD, stable slow MHD, and *unstable* slow MHD modes. Both studies put their emphases on the discovery and characterization of the discrete family, and didn't fully address the question of GMC formation in the context of non-uniform gravity. When an effective adiabatic index of the ISM is larger than a certain critical value, only the discrete family can have unstable solutions (Giz & Shu 1993; Kim *et al.* 1997). However, the growth time of the unstable *discrete* solution turned out to be about 10 times longer than that of the unstable *continuum* solution. It is, therefore, difficult

to explain formation of the GMCs by the discrete family of solutions.

In the present study we will concentrate on the continuum family of solutions. Since the external gravity is the driving force of the Parker instability, its time and length scales should depend on the nature of the Galactic gravity. This line of reasonings motivated us to seek a solution to the second problem of scales from the non-uniform nature of the Galactic gravity.

This paper is organized as follows. In §2 we first introduce three models for the Galactic gravity, and then construct equilibrium configuration for each of the gravity models. The MHD equations are linearized in the same section. In §3 dispersion relations are derived for the three gravity models, and the resulting sets of time and length scales are compared with each other. In §4 we summarize the paper with some discussions.

2. FORMULATION

Complete MHD equations for the magnetized gas and cosmic-ray particles under an externally given gravitational field are given by

$$\frac{\partial \rho}{\partial t} + \nabla \cdot (\rho \vec{v}) = 0, \quad (1)$$

$$\rho \left[\frac{\partial \vec{v}}{\partial t} + (\vec{v} \cdot \nabla) \vec{v} \right] = -\nabla \left(p + P + \frac{B^2}{8\pi} \right) + \frac{1}{4\pi} \vec{B} \cdot \nabla \vec{B} + \rho \vec{g}, \quad (2)$$

$$\frac{\partial \vec{B}}{\partial t} = \nabla \times (\vec{v} \times \vec{B}), \quad (3)$$

$$\frac{\partial p}{\partial t} + \vec{v} \cdot \nabla p + \gamma p \nabla \cdot \vec{v} = 0, \quad (4)$$

$$\vec{B} \cdot \nabla P = 0. \quad (5)$$

Here gas and cosmic-ray pressures are denoted by p and P , respectively. Other symbols have their usual meanings. Since the dispersion of random thermal velocities is much smaller than that of random cloud velocities, the main source of gas pressure is from the macroscopic turbulent motion of the clouds. To describe the local behavior of the Parker instability in the Galactic disk we introduce Cartesian coordinates x , y , and z , whose axes are taken to be parallel to the radial, azimuthal and vertical directions, respectively. The gravity has only vertical component, whose magnitude varies with height z , *i.e.* $\vec{g} = [0, 0, -g(z)]$.

If γ is larger than one and smaller than a critical value, the system becomes unstable by both families of continuum and discrete; if γ is less than one, there exists convective instability (Kim *et al.* 1997). Since our principal concern is to see the effects of gravity on the Parker instability, we simply choose $\gamma = 1$ and limit ourselves to the unstable continuum family of solutions.

2.1. Three Models for the Galactic Gravity

In the Galaxy the main source of gravity is stars, and the vertical gravity can be represented by

$$g_r(z) = 2 \frac{\langle v_*^2 \rangle}{H_*} \tanh\left(\frac{z}{H_*}\right), \quad (6)$$

where $\langle v_*^2 \rangle$ and H_* are the velocity dispersion and the scale height of the stars, respectively (Kim 1990; Giz & Shu 1993). We call this a realistic gravity as Giz & Shu did. In addition to this, we consider a uniform gravity,

$$g_u(z) = g_o \frac{z}{|z|}, \quad (7)$$

and a linear gravity,

$$g_l(z) = g' z, \quad (8)$$

where both g_o and g' are positive constants.

The uniform, linear and realistic gravity models are represented in Figure 1 by the dotted, dashed, and long-dashed lines, respectively. The two solid lines in the figure represent the strength of the gravitational accelerations of Oort (1965) and of BRC at solar neighborhood as functions of z . The gravity inferred from the distribution of K giants (Oort 1965) increases almost linearly up to $z \sim 500$ pc, beyond which it stays more-or-less constant. The same trend can be found from the gravity based on a galaxy model (BRC).

2.2. Unperturbed States

Let us suppose that initially an infinitely extended disk of gas and cosmic-ray particles is under the influences of magnetic and gravitational fields. The unperturbed magnetic field \vec{B}_o has only an azimuthal component, whose magnitude varies with z , *i.e.* $\vec{B}_o = [0, B_o(z), 0]$. Then the magnetohydrostatic equilibrium of the system is governed by

$$\frac{d}{dz} \left[p_o(z) + P_o(z) + \frac{B_o^2(z)}{8\pi} \right] = -\rho_o(z)g(z). \quad (9)$$

To close the differential equation, we take an isothermal equation of state for the gas pressure $p_o = a_s^2 \rho_o(z)$, where the velocity dispersion of clouds a_s^2 is assumed constant everywhere. We also assume that the ratio $\alpha = B_o^2/8\pi p_o$ of magnetic pressure to gas pressure and the ratio $\beta = P_o/p_o$ of cosmic-ray pressure to gas pressure are constants. Then, we have the same z -dependence for the unperturbed distributions of density, gas pressure, cosmic-ray pressure, and magnetic pressure as

$$\frac{\rho_o(z)}{\rho_o(0)} = \frac{p_o(z)}{p_o(0)} = \frac{P_o(z)}{P_o(0)} = \frac{B_o^2(z)}{B_o^2(0)} = \exp \left[-\frac{\Phi(z)}{(1 + \alpha + \beta)a_s^2} \right], \quad (10)$$

where $\Phi(z)$ is defined by

$$\Phi(z) \equiv \int_0^z g(z) dz, \quad (11)$$

and $\rho_o(0)$, $p_o(0)$, $P_o(0)$, and $B_o(0)$ denote their mid-plane values. An effective scale height H of the density distribution is defined by

$$2H \equiv \frac{1}{\rho_o(0)} \int_{-\infty}^{+\infty} \rho_o(z) dz. \quad (12)$$

Under the uniform gravity, the unperturbed state is described by an exponential function,

$$\frac{\rho_{o,u}(z)}{\rho_{o,u}(0)} = \frac{p_{o,u}(z)}{p_{o,u}(0)} = \frac{P_{o,u}(z)}{P_{o,u}(0)} = \frac{B_{o,u}^2(z)}{B_{o,u}^2(0)} = \exp\left[-\frac{|z|}{H}\right], \quad (13)$$

with the scale height being

$$H(\equiv H_u) = \frac{(1 + \alpha + \beta)a_s^2}{g_o}. \quad (14)$$

Under the linear gravity, the unperturbed state is given by a Gaussian function,

$$\frac{\rho_{o,l}(z)}{\rho_{o,l}(0)} = \frac{p_{o,l}(z)}{p_{o,l}(0)} = \frac{P_{o,l}(z)}{P_{o,l}(0)} = \frac{B_{o,l}^2(z)}{B_{o,l}^2(0)} = \exp\left[-\frac{\pi}{4} \left(\frac{z}{H}\right)^2\right], \quad (15)$$

where the scale height now becomes

$$H(\equiv H_l) = a_s \left[\frac{\pi(1 + \alpha + \beta)}{2g'} \right]^{\frac{1}{2}}. \quad (16)$$

For the case of the realistic gravity, it is described by

$$\frac{\rho_{o,r}(z)}{\rho_{o,r}(0)} = \frac{p_{o,r}(z)}{p_{o,r}(0)} = \frac{P_{o,r}(z)}{P_{o,r}(0)} = \frac{B_{o,r}^2(z)}{B_{o,r}^2(0)} = \text{sech}^{2s} \left(\frac{z}{H_*} \right), \quad (17)$$

where s is defined by

$$s \equiv \frac{\langle v_*^2 \rangle}{(1 + \alpha + \beta)a_s^2}. \quad (18)$$

If we call $(1 + \alpha + \beta)a_s^2$ as an *effective velocity dispersion* of clouds, then s is the ratio of the velocity dispersion of stars to the effective velocity dispersion of clouds. Substituting equation (17) into equation (12), we may describe the scale height of clouds in terms of H_* and s ,

$$H(\equiv H_r) = \frac{(2s - 2)!!}{(2s - 1)!!} H_* \equiv \frac{H_*}{h}, \quad (19)$$

where h is the ratio of the scale height of stars to that of clouds.

In order to specify the gravity models one should fix all the parameters g_o , g' , H_* , and $\langle v_*^2 \rangle$. Under each model of gravity, the magnetized gas and cosmic-ray particles adjust themselves to the equilibrium state. This means that the gravity parameters are related to the ISM parameters, α , β , H , and a_s (see eq. [14] for uniform gravity, eq. [16] for linear gravity, and eqs. [18] and [19] for realistic gravity). In practice, however, it is difficult to uniquely determine the values of g_o and g'

from either Oort’s (1965) or BRC’s gravity. Furthermore, the values of H_* and $\langle v_*^2 \rangle$ for one type of stars are different from those for other type of stars (Mihalas & Binney 1981). Therefore we decide to pin down the parameter values on the basis of the ISM conditions. They are specified in such a way that the gas scale height resulted from each of the three gravity models may all take the same value 160 pc that is known from observations (Falgarone & Lequeux 1973). In this way the comparison of the length and time scales among the three gravity models can be done on a common ground.

We take $\alpha = 0.25$ and $\beta = 0.4$, which are canonical values of the ISM (Spitzer 1978). For the scale height and the *rms* velocity of interstellar clouds we take 160 pc and 6.4 km s⁻¹, respectively (Falgarone & Lequeux 1973). Then, g_o and g' are equal to 1.4×10^{-9} cm s⁻², and 13.4×10^{-9} cm s⁻² kpc⁻¹. In addition to the above values of α , β , H , and a_s , we should also fix H_* and $\langle v_*^2 \rangle$ according to the chosen value of parameter s . This completes the specification of the realistic gravity model. The resulting three models are compared in Figure 1.

The parameter s defined by equation (18) is exactly the same as R in Giz & Shu (1993). They took $R \approx 3.5$ by fixing the value of $R_{\text{eq}} \approx 2$, ratio of the equivalent half-thickness of stellar disk to gas disk. But the equivalent half-thicknesses for various stellar objects in the Galaxy are different from type to type. In this paper, however, we will fix the s value in such a way that the resulting model of gravity may closely resemble the gravities of Oort (1965) and BRC. As can be seen from Figure 1, their gravities are reproduced by the realistic model with $s = 16$ and $s = 9$, respectively.

2.3. Linearized Perturbation Equations

We limit ourselves to the perturbations that are propagating in the plane defined by the azimuthal and vertical directions. In the two dimensional geometry the magnetic vector potential $\vec{A} = A(y, z)\hat{x}$ is more convenient to use than the magnetic field \vec{B} , because one scalar quantity, $A(y, z)$, is enough to specify the y and z components of the field. Taking the advantage we combine the linearized equations (1) through (5) into one for δA :

$$\begin{aligned}
 & -Q^2 \frac{\partial^2}{\partial t^2} \delta A + a_s^2 \left[(2\alpha + \gamma)Q^2 + \gamma^2 a_s^2 \frac{\partial^2}{\partial y^2} \right] \frac{\partial^2}{\partial z^2} \delta A \\
 & + \left\{ a_s^2 \left[2\alpha \frac{\partial^2}{\partial y^2} + \left(1 + \beta - \frac{\gamma}{2} \right) \frac{d^2}{dz^2} \ln \rho_o - \frac{1}{2} \left(\alpha + \frac{\gamma}{2} \right) \left(\frac{d}{dz} \ln \rho_o \right)^2 \right] Q^2 \right. \\
 & \left. + a_s^4 \left[\gamma \left(1 + \alpha + \beta - \frac{\gamma}{2} \right) \frac{d^2}{dz^2} \ln \rho_o - \left(1 + \alpha + \beta - \frac{\gamma}{2} \right)^2 \left(\frac{d}{dz} \ln \rho_o \right)^2 \right] \frac{\partial^2}{\partial y^2} \right\} \delta A = 0,
 \end{aligned} \tag{20}$$

where Q^2 is an acoustic wave operator defined by

$$Q^2 \equiv \frac{\partial^2}{\partial t^2} - \gamma a_s^2 \frac{\partial^2}{\partial y^2}. \tag{21}$$

If the following function

$$\delta A = f(z) \exp(i\omega t - ik_y y) \quad (22)$$

is substituted for the perturbation of vector potential, equation (20) becomes a second order ordinary differential equation

$$\begin{aligned} & a_s^2 \left[(2\alpha + \gamma)\omega^2 - 2\alpha\gamma a_s^2 k_y^2 \right] \frac{d^2 f}{dz^2} \\ & + \left\{ \omega^4 - a_s^2 \left[(2\alpha + \gamma)k_y^2 + \frac{1}{2} \left(\alpha + \frac{\gamma}{2} \right) \left(\frac{d}{dz} \ln \rho_o \right)^2 - \left(1 + \beta - \frac{\gamma}{2} \right) \left(\frac{d^2}{dz^2} \ln \rho_o \right) \right] \omega^2 \right\} f(z) \\ & + a_s^4 k_y^2 \left\{ 2\alpha\gamma k_y^2 - \left[(1 + \alpha + \beta)(1 + \alpha + \beta - \gamma) - \frac{1}{2}\alpha\gamma \right] \left(\frac{d}{dz} \ln \rho_o \right)^2 + \alpha\gamma \left(\frac{d^2}{dz^2} \ln \rho_o \right) \right\} f(z) = 0, \end{aligned} \quad (23)$$

where $f(z)$ is an amplitude function of the perturbation, ω is the angular frequency, and k_y is the wavenumber along the azimuthal direction.

As an upper boundary condition (BC), one may set $f = 0$ at $z = z_{\text{node}}$. The value of z_{node} can be either finite or infinite. As a lower BC, one may take either $f = 0$ or $df/dz = 0$ at $z = 0$. The former generates solutions having mirror symmetry; while the latter does the ones having antisymmetry. Since z -distribution of the unperturbed state has a cusp at the mid-plane under the uniform gravity (eq. [13]), only one condition, $f = 0$, is applicable to the lower boundary for the case of uniform gravity.

The effective scale height H and the crossing time over one scale height H/a_s are taken as normalization units of length and time. Dimensionless variables are then defined by

$$\Omega \equiv i\omega H/a_s, \quad \zeta \equiv z/H, \quad \nu_y \equiv k_y H. \quad (24)$$

The dimensionless vertical wavenumber, which depends on the lower BCs, should be defined by

$$\nu_z \equiv \begin{cases} 2\pi(H/2z_{\text{node}}) & \text{for symmetric modes} \\ 2\pi(H/4z_{\text{node}}) & \text{for antisymmetric modes.} \end{cases} \quad (25)$$

Since we used the same scale height H and the same *rms* velocity a_s for all the models, it is not necessary to distinguish the dimensionless variables from model to model.

3. TIME AND LENGTH SCALES

3.1. Uniform Gravity

In this paper we will re-derive dispersion relations for the Parker instability under the uniform gravity, because we want to point out the problems involved in the time and the length scales, and because the results from the uniform model comprise a comparison basis. Under the uniform

gravity $d \ln \rho_o(z)/dz$ and $d^2 \ln \rho_o(z)/dz^2$ in equation (23) should be replaced by $-1/H$ and 0, respectively (see eq. [13]). In terms of the dimensionless variables, it takes the form

$$\begin{aligned} & \left[(2\alpha + \gamma)\Omega^2 + 2\alpha\gamma\nu_y^2 \right] \frac{d^2 f_u}{d\zeta^2} + \left\{ -\Omega^4 - (2\alpha + \gamma) \left(\nu_y^2 + \frac{1}{4} \right) \Omega^2 \right. \\ & \left. - 2\alpha\gamma\nu_y^4 + \left[(1 + \alpha + \beta)(1 + \alpha + \beta - \gamma) - \frac{1}{2}\alpha\gamma \right] \nu_y^2 \right\} f_u = 0, \end{aligned} \quad (26)$$

which is what Parker(1966) gave in his Appendix III. Because the coefficients of $d^2 f_u/d\zeta^2$ and f_u are constants, and because only symmetric BC at $\zeta = 0$ should be applied to the model of the uniform gravity, we may set $f_u \propto \sin(\nu_z \zeta)$. Then, an equation for the dispersion relation can be written

$$\begin{aligned} & \Omega^4 + (2\alpha + \gamma) \left(\nu_y^2 + \nu_z^2 + \frac{1}{4} \right) \Omega^2 \\ & + \left\{ 2\alpha\gamma(\nu_y^2 + \nu_z^2) - \left[(1 + \alpha + \beta)(1 + \alpha + \beta - \gamma) - \frac{1}{2}\alpha\gamma \right] \right\} \nu_y^2 = 0. \end{aligned} \quad (27)$$

The resulting dispersion relations are shown in Figure 2. The perturbation with a finite vertical wavelength grows less rapidly than the one with an infinite wavelength. If we take $H = 160$ pc, $\nu_z = 1.0$ corresponds to $z_{\text{node}} \simeq 500$ pc. Since the scale heights of interstellar clouds and inter-cloud gas are 160 pc and 300 pc (Falgarone and Lequeux 1973), respectively, 500 pc is a reasonable choice for the nodal point (e.g., Elmegreen 1982). For the perturbation with the infinite vertical wavelength, the minimum growth time of our result is 5.5×10^7 years and Parker's (1966) estimate is 3×10^7 years. Besides detailed values of α and β that went into these estimates, the time scale of $3 \sim 6 \times 10^7$ years is a gross under-estimate; under the Galactic environments it seems unrealistic to think of perturbations whose vertical wavelength is much larger than the scale height of the cloud distribution itself. In the case of $\nu_z = 1.0$, the time and length scales become 1.2×10^8 years and 1.6 kpc, respectively. The growth time, 1.2×10^8 years, is much longer than the lifetime of GMCs, 3×10^7 years (Blitz and Shu 1980), and the length scale, 1.6 kpc, is larger than the mean separation of the GMCs, 0.5 kpc (Blitz 1991).

Figure 3 illustrates the detailed dependences of the the minimum growth time upon the parameters α and β . In most region of the (α, β) plane the growth time turns out to be longer than the cloud lifetime. From the illustration we conclude that under the uniform gravity the Parker instability may not play any significant roles in the formation of GMCs. The growth time becomes comparable to the lifetime of GMCs only in a limited region of the parameter plane, where α and β take unacceptably high values for the general ISM. This is exactly the reason why Mouschovias *et al.* (1974) invoked the dense region of Galactic shocks as an onset place of the Parker instability.

3.2. Linear Gravity

Under the linear gravity, $d \ln \rho_{o,l}(z)/dz$ becomes $-(\pi/2)(z/H^2)$ (see eq. [15]). After substituting it and its gradient into equation (23), we can write the resulting equation in the following dimensionless form:

$$\frac{d^2 f_l}{d\zeta^2} + (E_l - V_{o,l} \zeta^2) f_l = 0, \quad (28)$$

where E_l and $V_{o,l}$ are given by

$$E_l = \frac{\pi}{4} - \frac{\Omega^4 + [(2\alpha + \gamma)\nu_y^2 + \frac{\pi}{2}(1 + \alpha + \beta)]\Omega^2 + 2\alpha\gamma\nu_y^4}{(2\alpha + \gamma)\Omega^2 + 2\alpha\gamma\nu_y^2}, \quad (29)$$

$$V_{o,l} = \frac{\pi^2}{4} \left[\frac{1}{4} - \frac{(1 + \alpha + \beta)(1 + \alpha + \beta - \gamma)\nu_y^2}{(2\alpha + \gamma)\Omega^2 + 2\alpha\gamma\nu_y^2} \right]. \quad (30)$$

To derive the dispersion relation we will use the same method given in the Appendix of Kim *et al.* (1997).

Kim *et al.* (1997) showed that, under the linear gravity, the dispersion relation for the continuum family of solutions with a mirror symmetric lower BC are nearly the same as that with an antisymmetric BC. Under the point-mass-dominated gravity, however, the antisymmetric modes grow faster than the symmetric ones (Horiuchi *et al.* 1988). Such difference in the behavior of growth rate stems from the difference in the nature of the chosen gravity models. The growth rate under the point-mass-dominated gravity is sensitive to the lower BCs, because the gravity has its maximum close to the lower boundary. On the contrary the growth rates under the linear and realistic gravities are insensitive to the lower BCs, because these models have their maxima at far from the mid-plane. So in this paper we present the dispersion relations only for the symmetric lower BC.

In the linear model the vertical acceleration increases with z without a bound, while in the Galaxy it approaches a finite value at large distance from the mid-plane. We should, therefore, limit the disk extent within a finite height from the central plane. The dispersion relations shown in Figure 4 are for the perturbations with $\nu_z = 0.5$ and $\nu_z = 1.0$. This figure clearly indicates a strong dependence of the growth rate on the vertical wavenumber. We think $\nu_z = 1.0$ a realistic choice for the Galaxy. With the same parameters that are used in Figure 2, the perturbation of maximum growth rate has a horizontal wavelength 340 pc and a minimum growth time 1.5×10^7 years.

The linear gravity drives the Parker instability much faster than the uniform gravity. By almost an order of magnitude reduction is achieved in the growth time scale, even with the perturbation wavelength as short as 340 pc. Such reduction is possible for a wide range of α and β values. This can be seen from the contours, in Figure 5, of equal minimum growth times traced out in the (α, β) plane. Comparison of the two sets of figures (Figs. 2 and 3 versus Figs. 4 and 5) indicates that the growth rate is indeed sensitive to the nature of the externally given gravitational fields.

3.3. Realistic Gravity

Using the unperturbed state expressed by equation (17) together with the definition of h (eq. [19]), we may express the perturbation equation (23) in the form

$$\frac{d^2 f_r}{d\zeta^2} + \left[E_r - V_{o,r} \operatorname{sech}^2 \left(\frac{\zeta}{h} \right) \right] f_r = 0, \quad (31)$$

with

$$E_r = (G_3 + G_4)/G_1, \quad (32)$$

$$V_{o,r} = (G_3 - G_2)/G_1, \quad (33)$$

where G_1 , G_2 , G_3 , and G_4 are given by

$$G_1 = (2\alpha + \gamma)\Omega^2 + 2\alpha\gamma\nu_y^2, \quad (34)$$

$$G_2 = \left[-(2 + 2\beta - \gamma)\Omega^2 + 2\alpha\gamma\nu_y^2 \right] \frac{s}{h^2}, \quad (35)$$

$$G_3 = \left\{ -(2\alpha + \gamma)\Omega^2 + [4(1 + \alpha + \beta)(1 + \alpha + \beta - \gamma) - 2\alpha\gamma]\nu_y^2 \right\} \frac{s^2}{h^2}, \quad (36)$$

$$G_4 = -\Omega^4 - (2\alpha + \gamma)\nu_y^2\Omega^2 - 2\alpha\gamma\nu_y^4. \quad (37)$$

To evaluate the dispersion relations we again use the method explained in the Appendix of Kim *et al.* (1997).

The resulting dispersion relations of the symmetric mode are shown in Figure 6 for different values of s . The larger the s value is, the more unstable the system becomes. This is because the gravity with a larger value of s is stronger than that with a smaller one (see Fig. 1). To show the effect of the vertical wavenumber on the growth rate, the dispersion relations for the cases of $\nu_z = 0.0, 0.5$, and 1.0 are compared to each other in Figure 7. The smaller the vertical wavenumber or the longer the vertical wavelength is, the faster the instability grows. For the set of parameters $s = 9, \nu_z = 1, \alpha = 0.25, \beta = 0.4$, and $\gamma = 1$, the minimum growth time becomes 1.8×10^7 years and the corresponding wavelength is 400 pc. If $s = 16$ is taken with the other parameters being fixed at the same values, the time and length scales are slightly reduced. Figure 8 shows the equi-growth time contours in the (α, β) plane for the case of $\gamma = 1, \nu_z = 1$, and $s = 9$. Under the realistic gravity the growth time becomes shorter than the GMC lifetime for most range of the α and β values.

3.4. Comparison of Time and Length Scales

The dispersion relations resulting from the three models of gravity are compared in Figure 9. The same set of parameter values, $\alpha = 0.25, \beta = 0.4, \gamma = 1.0, \nu_z = 1.0$, is used for all the three models. To do a good justice in the comparison, the time and length scales of the three models

are normalized by using the same set of effective scale height 160 pc and *rms* velocity 6.4 km s⁻¹. The vertical wavenumber $\nu_z = 1$ places a nodal point at $z \simeq 500$ pc. Among the three the linear gravity gives the strongest acceleration near the nodal point; while the uniform gravity does the weakest (see Fig. 1). Since it is the external gravity that drives the Parker instability, the growth rates for the linear gravity are generally higher than for the other two.

Table 1 lists the minimum growth times and their length scales for each of the three gravity models. We include the scales for both the symmetric and antisymmetric modes. The parameters used in the calculation of these scales are the same as those in Figure 9. The length scale corresponds to the inter-distance of the condensations that would be formed by the Parker instability. So the length scale for the symmetric mode, which is equal to the perturbation wavelength, is twice the value for the antisymmetric one. We should also clarify the vertical wavenumber used for the antisymmetric modes. As is done for the symmetric modes, the upper nodal point is set at $z \simeq 500$ pc for the antisymmetric ones. Since the antisymmetric mode doesn't have a nodal point at $z = 0$, this choice corresponds to the vertical wavenumber $\nu_z = 0.5$, which is smaller by a factor of two than that for the symmetric one. It is, however, fair to use the scales with the same upper node rather than those with the same vertical wavenumber. This point should be kept in mind, when one compares the scales of the time and length for the symmetric modes with those for the antisymmetric ones.

In spite of the incompatibility of the antisymmetric mode with the uniform gravity, we have listed, in Table 1, the time and length scales for the antisymmetric mode, because the incompatibility stems from an over-simplification of the Galactic gravity, and because we want to compare the scales from different models of gravity. Since the realistic gravity model with $s = 9$ represents the results of BRC fairly well, we take 1.8×10^7 years for the growth time scale and 400 pc (200 pc) for its length scale of the symmetric (antisymmetric) mode of the Parker instability. These time and length scales are about 1/7 and 1/4 of those for the uniform gravity, respectively.

4. SUMMARY AND DISCUSSION

To investigate the effect of external gravity on the continuum family solutions of the Parker instability, we introduce uniform, linear, and realistic models for the Galactic gravity. The gravity models are specified by fixing the ratio α of magnetic pressure to gas pressure at 0.25, the ratio β of cosmic-ray pressure to gas pressure at 0.4, the *rms* velocity $\langle a_s^2 \rangle^{1/2}$ of interstellar clouds at 6.4 km s⁻¹, and the effective scale height H of cloud distribution at 160 pc. For the realistic model based on the hyperbolic tangent function, we need to specify one more parameter s , which is the ratio of the velocity dispersion of stars to the effective velocity dispersion of clouds (see eq. [18]). The Galactic gravities of Oort (1965) and BRC at solar neighborhood are reproduced by the realistic model with $s = 16$ and $s = 9$, respectively.

Under the uniform gravity the time and length scales of symmetric mode solution are 1.2×10^8

years and 1.6 kpc; while they become 1.8×10^7 years and 400 pc under the realistic gravity with $s = 9$. Under the linear and realistic gravities the antisymmetric modes grow at almost the same rate as the symmetric mode. However, as for the separation of condensations, the length scale of the antisymmetric mode becomes, of course, a half of the symmetric mode's. Changing the nature of gravity from uniform to realistic has thus reduced the time and length scales in the Galactic environments by factors of 7 and 4, respectively. Therefore, it is not necessary to invoke high values of α and β to reduce the scales.

The rotation of the Galactic disk is known to exercise a stabilizing effect on the Parker instability (Foglizzo & Tagger 1994). With the uniform gravity Zweibel & Kulsrud (1975) found that the rigid body rotation would increase, over the non-rotating case, the growth time by a factor of two. With a gravity model based on a combination of linear and hyperbolic tangent functions, which is very close to ours, Hanawa *et al.* (1992b) found that the rigid body rotation would increase the growth time by factors of 1.3 to 7.5 for α varying from 1.0 to 0.1. They placed the upper boundary of the Galactic disk at $z = 200$ pc, while we did at 500 pc. Because the external gravity drives the gas to slide down the field lines from top part of the disk first, the growth rate one obtains from linear stability analysis depends rather sensitively on the magnitude of acceleration at the upper boundary. The acceleration at $z = 200$ pc is about two thirds of its value at $z = 500$ pc. Therefore, an increase in the growth time the rotation would bring to our case may not be so large as their findings. Furthermore, they didn't include cosmic-ray particles as an ISM constituent. Since the "light" cosmic-rays drive the field lines to buckle mainly upward, a triggering of the instability by the cosmic-ray pressure doesn't seem to be seriously affected by the Galactic rotation. If the Galactic rotation had been included in our analysis with the non-uniform gravities, the growth time would have increased by a factor of 2 or 3 for moderate values of α and β . However, for very low values of α and β , the rotation is very likely to make the growth time longer than the GMC lifetime (Figure 8).

Are the GMCs formed by the Parker instability? As far as the time and length scales are concerned, our linear stability analysis done with the realistic gravity model gives a positive answer to the question. To have a better answer we should also know how much enhancement in density can be made by the Parker instability. From the linear analysis alone one may not have information on the density enhancement factor. Very recently Basu *et al.* (1996; 1997) performed two-dimensional simulations of the Parker instability under the uniform gravity. The density enhancement they obtained at the mid-plane amounts to a factor of only 2. Under the non-uniform gravity the enhancement factor may not be much larger than 2, because the acceleration of any realistic gravity models anyhow approaches zero near the mid-plane. As for the density enhancement the answer is likely to be a negative one. The GMCs may have formed through a cooperative interplay of the Parker and Jeans instabilities.

We thank Dr. D. Ryu for making useful suggestions and to a referee, Dr. T. Foglizzo, for giving us many constructive comments. SSH wishes to acknowledge the financial support from the

Korea Research Foundation made in the year of 1997. JK was supported by the Korean Ministry of Science and Technology through the Korea Astronomy Observatory grant 97-5400-000.

Table 1. Comparison of Time and Length Scales

scales	uniform		linear		realistic ($s = 9$)	
	symmetric	antisymmetric*	symmetric	antisymmetric	symmetric	antisymmetric
time [year]	1.2×10^8	1.2×10^8	1.5×10^7	1.5×10^7	1.8×10^7	1.8×10^7
length [pc]	1600	800	340	170	400	200

*Incompatible with the exponential distribution of the unperturbed state

REFERENCES

- Appenzeller, I. 1974, *A&A*, 36, 99.
- Asséo, E., Cesarsky, C. J., Lachièze-Rey, M., & Pellat, R. 1980, *ApJ*, 237, 752.
- Basu, S., Mouschovias, T. Ch., & Paleologou, E. V. 1996, *Astro. Lett. and Comm.*, 34, 333.
- Basu, S., Mouschovias, T. Ch., & Paleologou, E. V. 1997, *ApJ*, 480, L55.
- Bienaymé, O., Robin, A. C., & Crézé, M. 1987, *A&A*, 180, 94 (BRC).
- Blitz, L. 1991, in *Physics of Star Formation and Early Stellar Evolution*, ed. C. J. Lada & N. D. Kylafis (Dordrecht: Kluwer), 3.
- Blitz, L., & Shu, F. H. 1980, *ApJ*, 238, 148.
- Elmegreen, B. G. 1982, *ApJ*, 253, 634.
- Falgarone, E., & Lequeux, J. 1973, *A&A*, 25, 253.
- Foglizzo, T., & Tagger, M. 1994, *A&A*, 287, 297.
- Giz, A. T., & Shu, F. H. 1993, *ApJ*, 404, 185.
- Gomez de Castro, A. I., & Pudritz, R. E. 1992, *ApJ*, 395, 501.
- Handa, T., Sofue, Y., Ikeuchi, S., Kawabe, R., & Ishizuki, S. 1992, *PASJ*, 44, L227.
- Hanawa, T., Matsumoto, R., & Shibata, K. 1992a, *ApJ*, 393, L71.
- Hanawa, T., Nakamura, F., & Nakano, T. 1992b, *PASJ*, 44, 509.
- Horiuchi, T., Matsumoto, R., Hanawa, T., & Shibata, K. 1988, *PASJ*, 40, 147.
- Kamaya, H., Mineshige, S., Shibata, K., & Matsumoto, R. 1996, *ApJ*, 458, L25.
- Kamaya, H., Horiuchi, T., Matsumoto, R., Hanawa, T., Shibata, K., & Mineshige, S. 1997, *ApJ*, 486, 307.
- Kim, J. 1990, Master's thesis, Seoul National University.
- Kim, J., Hong, S. S., & Ryu, D. 1997, *ApJ*, 485, 228.
- Kim, J., Hong, S. S., Ryu, D., & Jones, T. W. 1998, *ApJ*, submitted.
- Mihalas, D., & Binney, J. 1981, *Galactic Astronomy* (San Francisco: Freeman), 423.
- Mouschovias, T. Ch., Shu, F. H., & Woodward P. R. 1974, *A&A*, 33, 73.

- Nakamura, F., Hanawa, T., & Nakano, T. 1991, PASJ, 43, 685.
- Oort, J. H. 1965, in *Galactic Structure*, ed. A. Blaauw & M. Schmidt(Chicago: Univ. of Chicago Press), 455.
- Parker, E. N. 1966, ApJ, 145, 811.
- Parker, E. N. 1967, ApJ, 149, 535.
- Shibata, K., & Matsumoto, R. 1991, Nature, 353, 633.
- Shu, F. H. 1974, A&A, 33, 55.
- Spitzer, L., Jr. 1978, *Physical Processes in the Interstellar Medium* (New York: Wiley), 226.
- Tout, C. A., & Pringle, J. E. 1992, MNRAS, 259, 604.
- Zweibel, E. G., & Kulsrud, R. M. 1975, ApJ, 201, 63.

Fig. 1.— Vertical acceleration at solar neighborhood. The two solid lines represent the results of Oort (1965) and of Bienaymé, Robin & Crézé (1987). A dotted line, a dashed line, and three long-dashed lines are for the models of uniform, linear, and realistic gravities, respectively. The parameter s is the ratio of the velocity dispersion of stars to the effective velocity dispersion of clouds.

Fig. 2.— Dispersion relations of the Parker instability under the uniform gravity. Each curve is marked by the value of vertical wavenumber. $\nu_z = 0.0$ corresponds to an infinite wavelength. If the density scale height of clouds is 160 pc, $\nu_z = 0.5$ and $\nu_z=1.0$ have nodal points at $\simeq 1000$ pc and $\simeq 500$ pc, respectively. The ordinate represents square of the normalized growth rate, and the abscissa does the normalized horizontal wavenumber. The effective adiabatic index γ , the ratio α of magnetic to gas pressure, and the ratio β of cosmic-ray to gas pressure are specified within the frame.

Fig. 3.— Loci of equi-growth time are traced out in the (α, β) plane for the Parker instability under the uniform gravity.

Fig. 4.— Dispersion relations of the Parker instability under the linear gravity. Each curve is marked by the vertical wavenumber ν_z . The ordinate represents square of the normalized growth rate, and the abscissa the normalized horizontal wavenumber. The system parameters used in the calculation are given in the frame.

Fig. 5.— Loci of equi-growth time are traced out in the (α, β) plane for the Parker instability under the linear gravity.

Fig. 6.— Dispersion relations of the Parker instability under the realistic gravity. Each curve is marked by the value of s , which is the ratio of the velocity dispersion of stars to the effective velocity dispersion of clouds. The ordinate represents square of the normalized growth rate, and the abscissa the normalized horizontal wavenumber. The system parameters are specified within the frame.

Fig. 7.— Dispersion relations of the Parker instability under the realistic gravity. Each curve is marked by the vertical wavenumber ν_z . The ordinate represents square of the normalized growth rate, and the abscissa the normalized horizontal wavenumber. The system parameters are given in the frame.

Fig. 8.— Loci of equi-growth time are traced out in the (α, β) plane for the Parker instability under the realistic gravity.

Fig. 9.— Dispersion relations of the uniform, linear, and realistic gravities are compared with each other. The ordinate represents square of the normalized growth rate, and the abscissa the normalized horizontal wavenumber. The system parameters are specified in the frame.

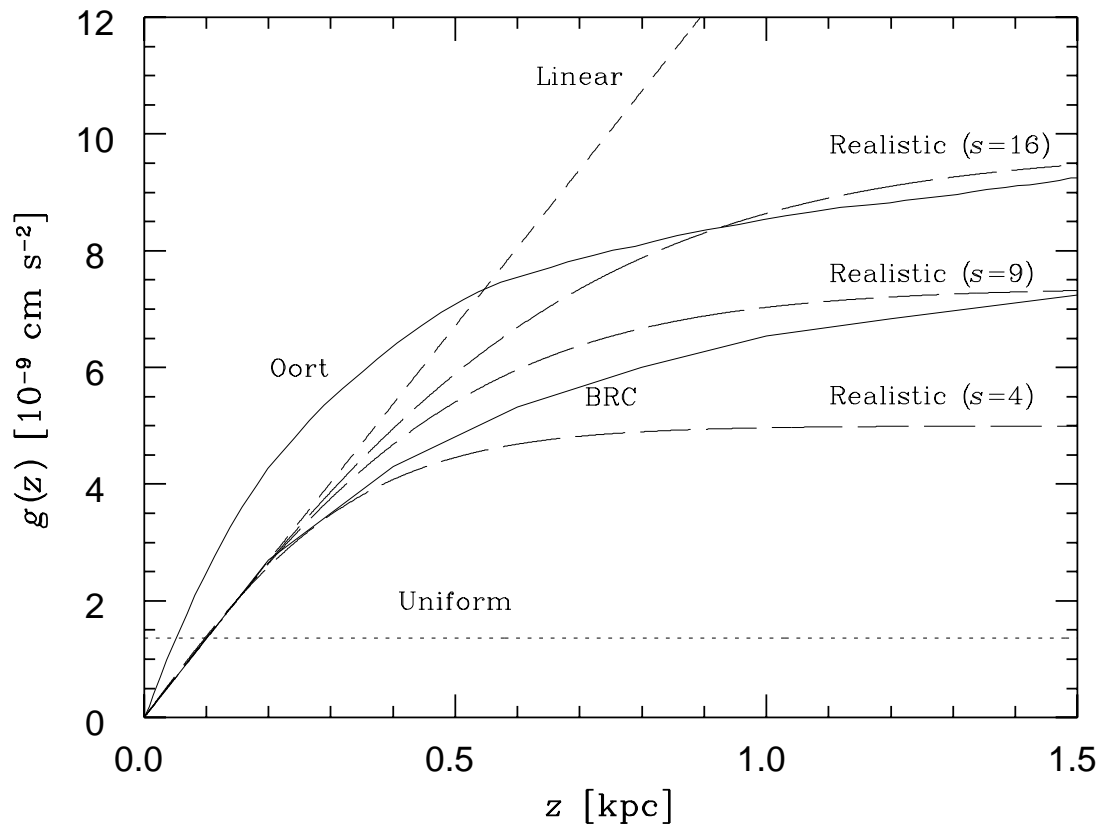


Figure 1

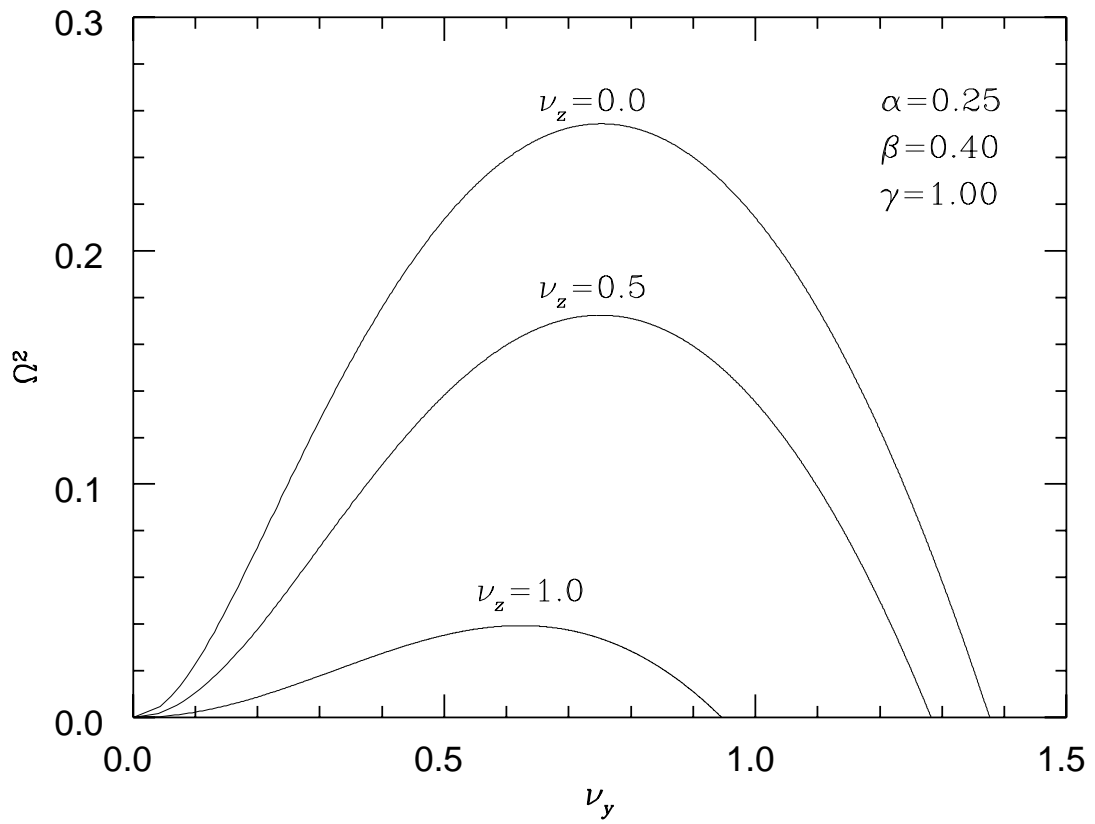


Figure 2

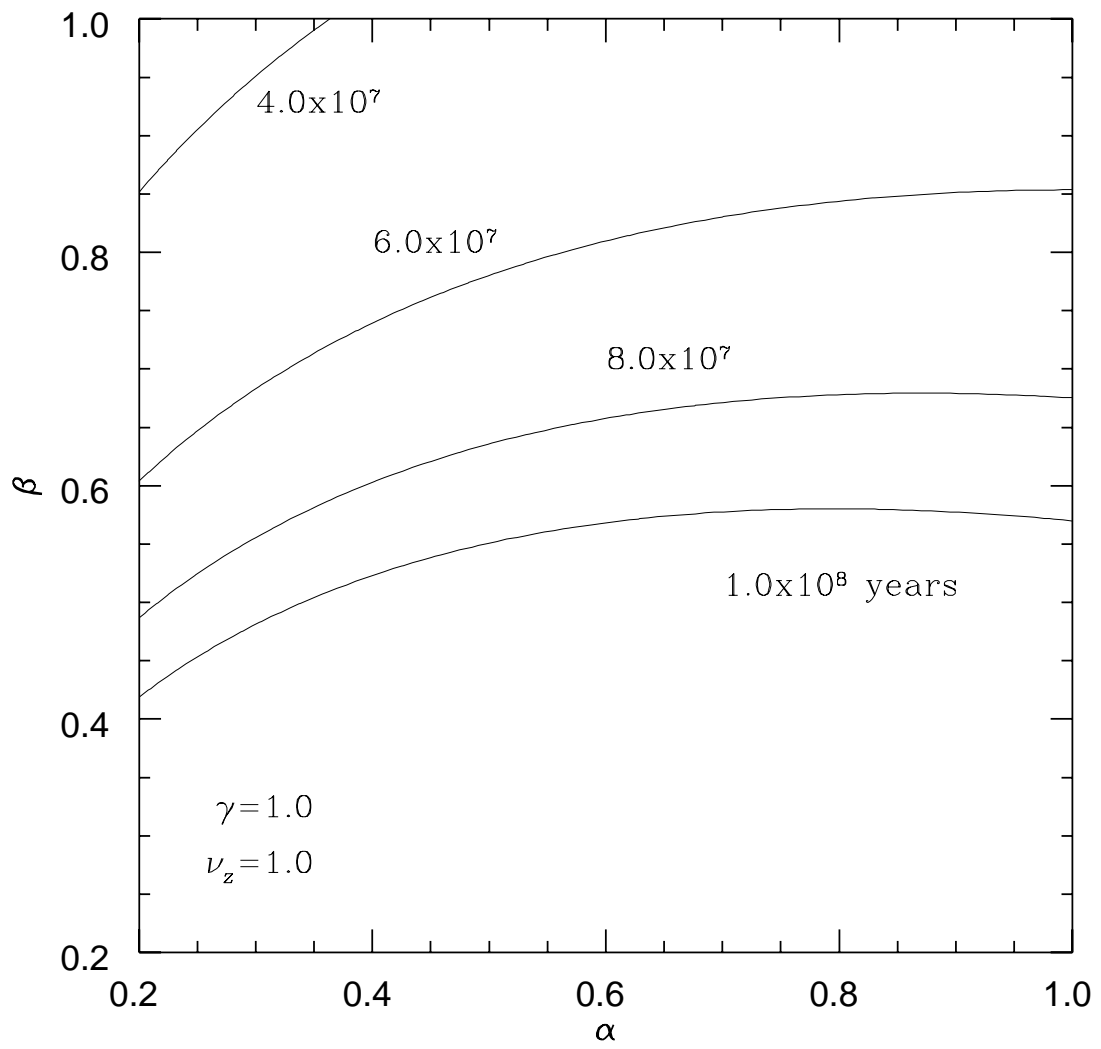


Figure 3

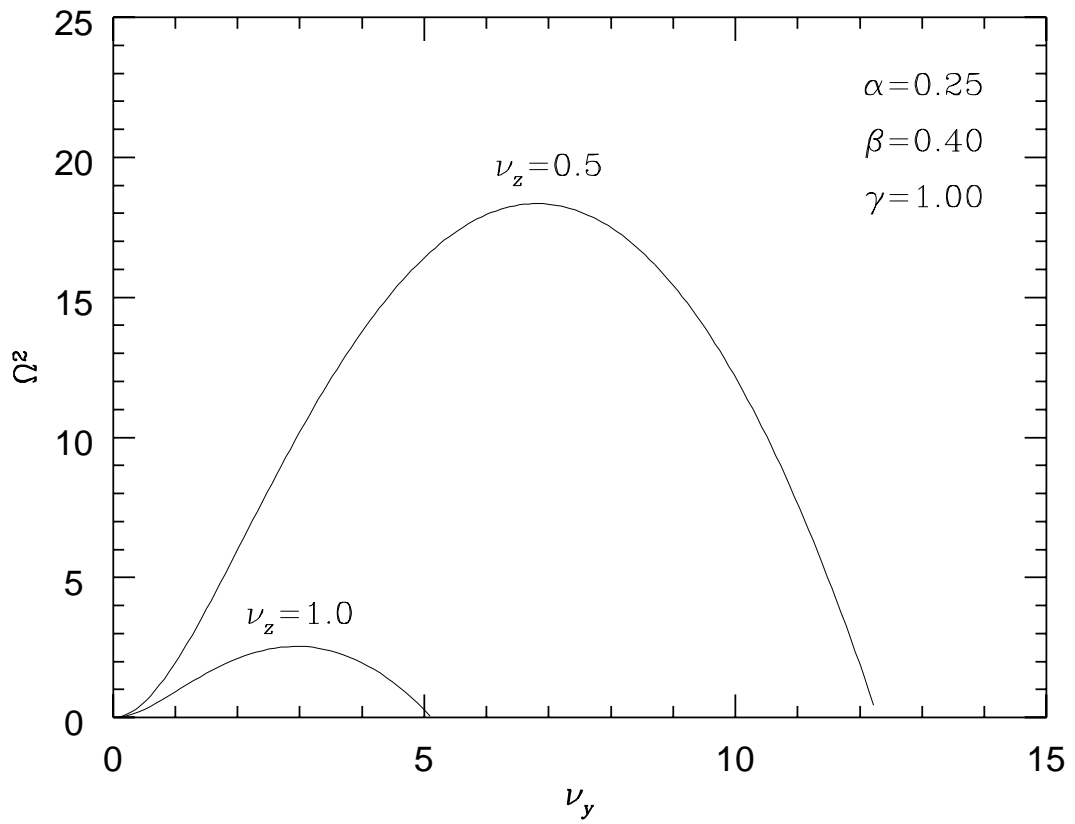


Figure 4

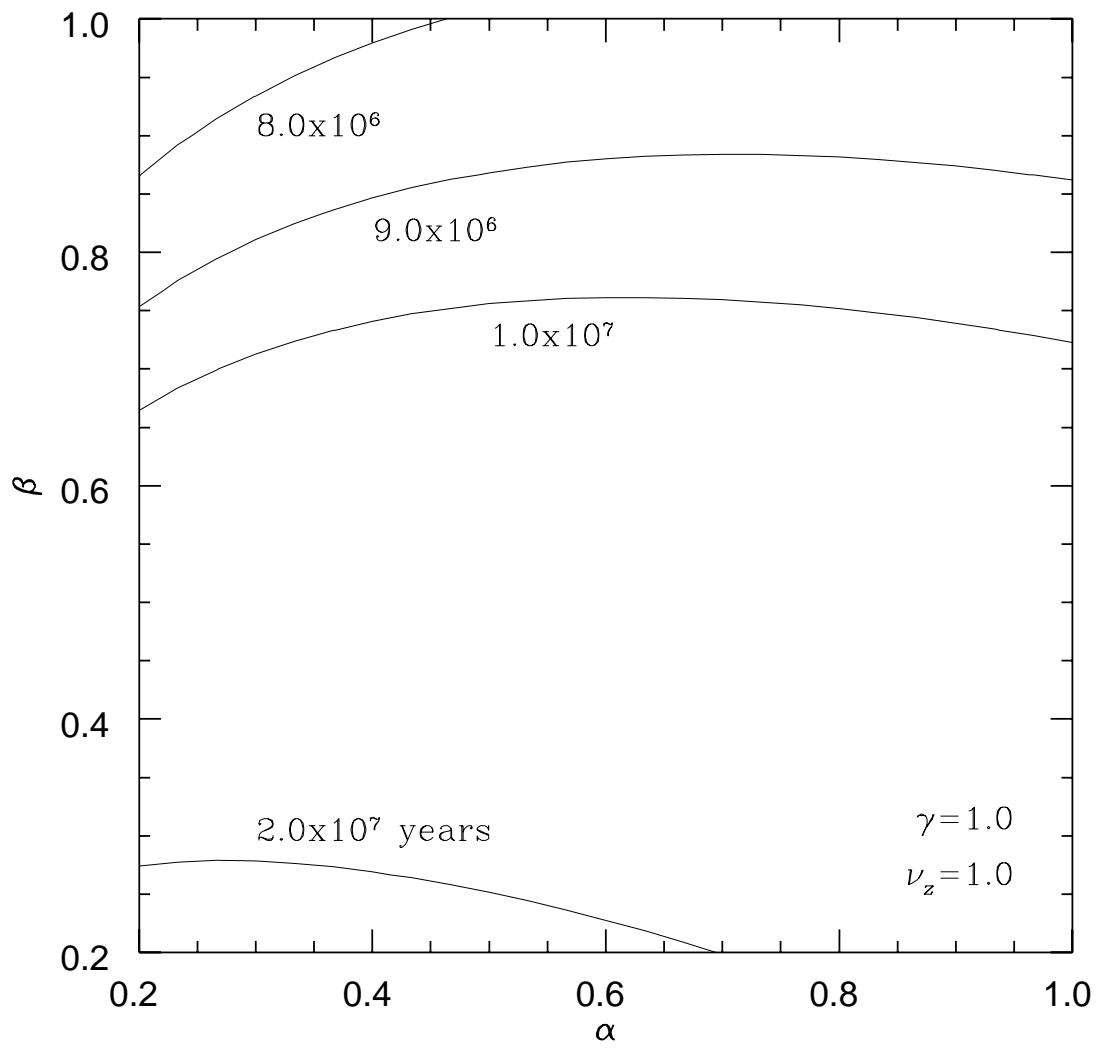


Figure 5

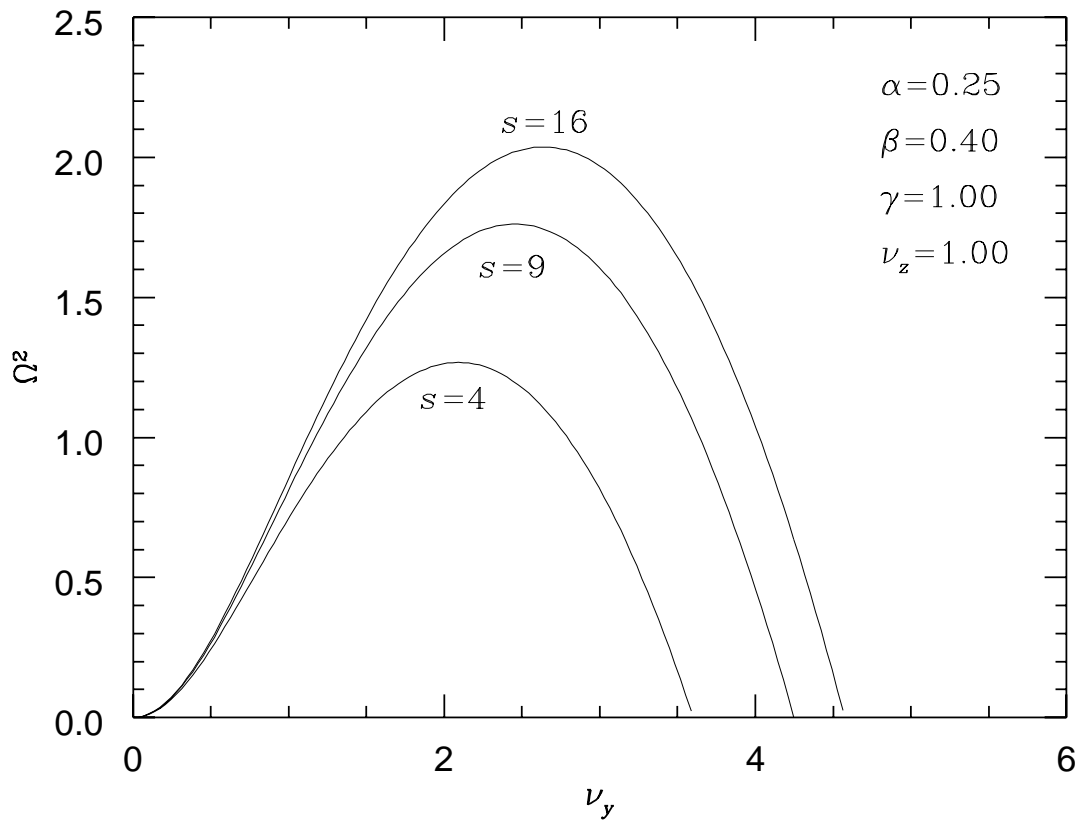


Figure 6

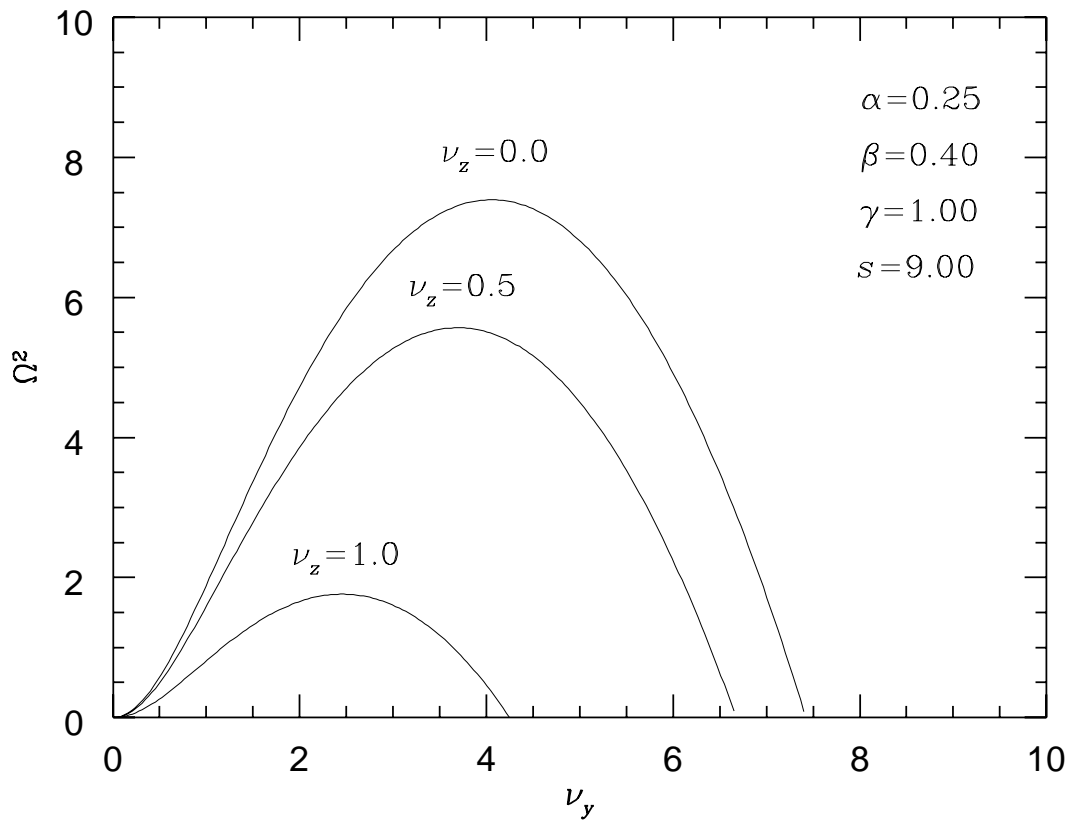


Figure 7

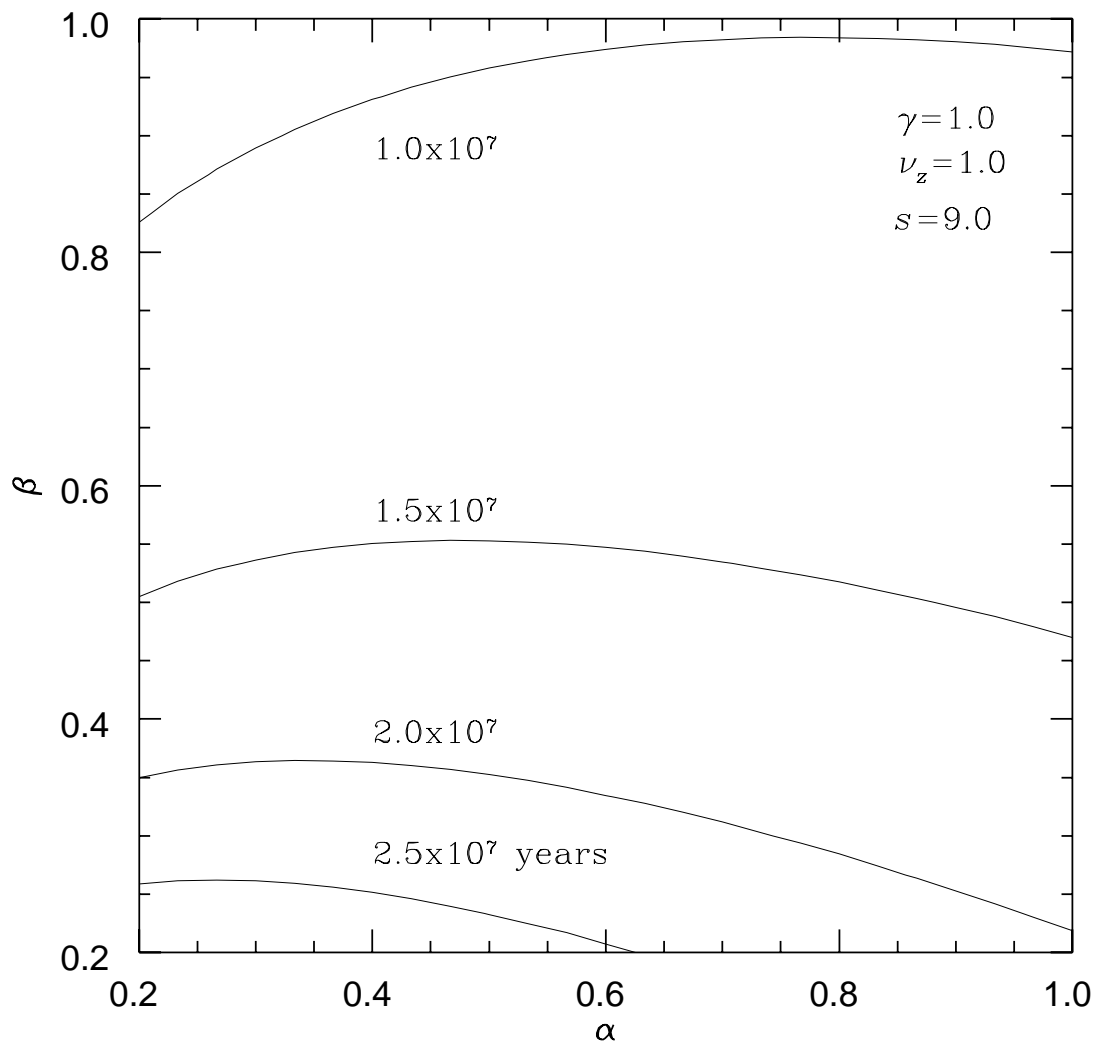


Figure 8

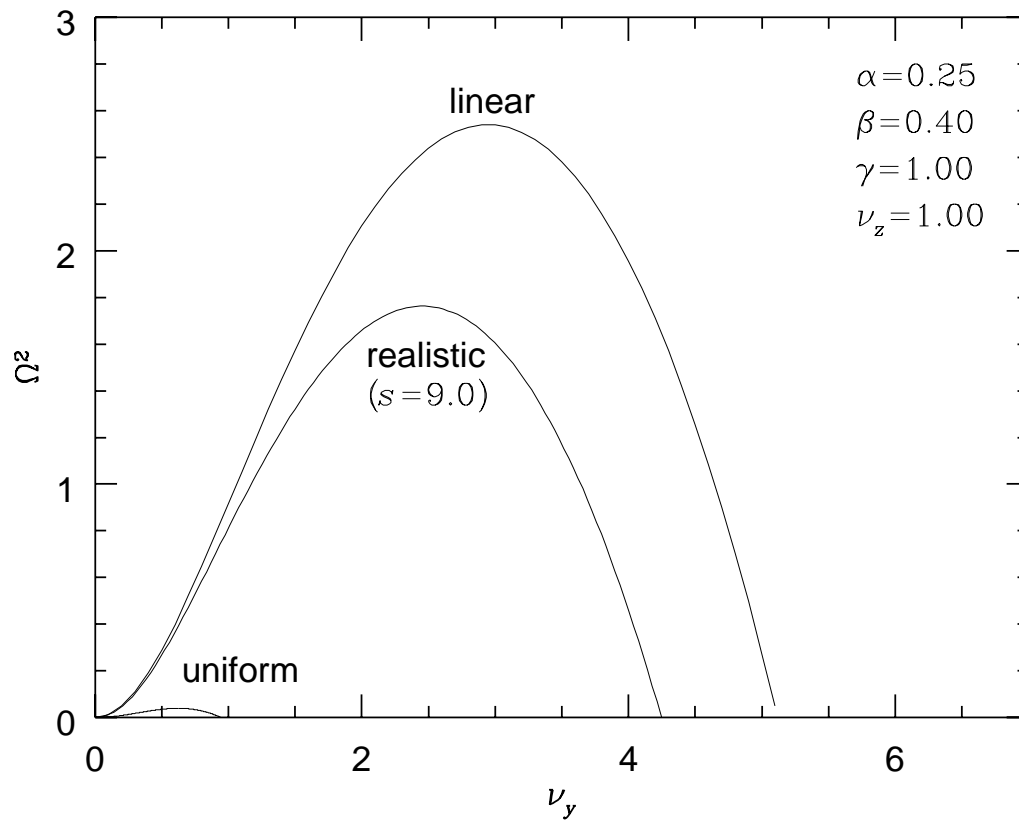


Figure 9